Vertical optical antennas integrated with spiral ring gratings for large local electric field enhancement and directional radiation

Baoan Liu,[1] Dongxing Wang,[2] Chuan Shi,[1] Kenneth B. Crozier,[2] and Tian Yang[1]*

[1]*University of Michigan – Shanghai Jiao Tong University Joint Institute, National Key Laboratory of Nano/Micro Fabrication Technology, Key Laboratory for Thin Film and Microfabrication of the Ministry of Education, State Key Lab of Advanced Optical Communication Systems and Networks, Shanghai Jiao Tong University, Shanghai 200240, China*

[2]*School of Engineering and Applied Sciences, Harvard University, Cambridge, Massachusetts 02138, USA*

**tianyang@sjtu.edu.cn*

Abstract: We propose a device for reproducible achievement of enormous enhancement of local electric field intensities. In each device, a metallic spiral ring grating is employed for efficient excitation of local surface plasmon resonance in the tiny gap of a vertically oriented optical antenna. Radiation from the optical antenna is collimated by the ring grating which facilitates efficient collection. As a numerical example, for a gold nanosphere placed one nanometer above the center of a gold spiral ring grating, our simulations predict an increase in local electric field intensity of up to seven orders of magnitude compared to planewave illumination, and collection efficiencies of up to 68% by an objective with a numerical aperture of 0.7. Single molecule SERS application is discussed.

OCIS codes: (050.1950) Diffraction gratings; (240.6680) Surface plasmons; (240.6695) Surface-enhanced Raman scattering.

References and links

1. W. L. Barnes, A. Dereux, and T. W. Ebbesen, "Surface plasmon subwavelength optics," Nature **424**(6950), 824–830 (2003).
2. S. A. Maier, M. L. Brongersma, P. G. Kik, S. Meltzer, A. A. G. Requicha, and H. A. Atwater, "Plasmonics—a route to nanoscale optical devices," Adv. Mater. (Deerfield Beach Fla.) **13**(19), 1501–1505 (2001).
3. K. Kneipp, Y. Wang, H. Kneipp, L. T. Perelman, I. Itzkan, R. R. Dasari, and M. S. Feld, "Single molecule detection using surface-enhanced raman scattering (SERS)," Phys. Rev. Lett. **78**(9), 1667–1670 (1997).
4. J. Jiang, K. Bosnick, M. Maillard, and L. Brus, "Single molecule raman spectroscopy at the junctions of large ag nanocrystals," J. Phys. Chem. B **107**(37), 9964–9972 (2003).
5. C. E. Talley, J. B. Jackson, C. Oubre, N. K. Grady, C. W. Hollars, S. M. Lane, T. R. Huser, P. Nordlander, and N. J. Halas, "Surface-enhanced Raman scattering from individual au nanoparticles and nanoparticle dimer substrates," Nano Lett. **5**(8), 1569–1574 (2005).
6. A. Bek, R. Jansen, M. Ringler, S. Mayilo, T. A. Klar, and J. Feldmann, "Fluorescence enhancement in hot spots of AFM-designed gold nanoparticle sandwiches," Nano Lett. **8**(2), 485–490 (2008).
7. J. P. Camden, J. A. Dieringer, Y. Wang, D. J. Masiello, L. D. Marks, G. C. Schatz, and R. P. Van Duyne, "Probing the structure of single-molecule surface-enhanced Raman scattering hot spots," J. Am. Chem. Soc. **130**(38), 12616–12617 (2008).
8. H. Xu, J. Aizpurua, M. Käll, and P. Apell, "Electromagnetic contributions to single-molecule sensitivity in surface-enhanced raman scattering," Phys. Rev. E Stat. Phys. Plasmas Fluids Relat. Interdiscip. Topics **62**(3 3 Pt B), 4318–4324 (2000).
9. E. Hao and G. C. Schatz, "Electromagnetic fields around silver nanoparticles and dimers," J. Chem. Phys. **120**(1), 357–366 (2004).
10. J. M. McMahon, A.-I. Henry, K. L. Wustholz, M. J. Natan, R. G. Freeman, R. P. Duyne, and G. C. Schatz, "Gold nanoparticle dimer plasmonics: finite element method calculations of the electromagnetic enhancement to surface-enhanced Raman spectroscopy," Anal. Bioanal. Chem. **394**(7), 1819–1825 (2009).
11. K. B. Crozier, A. Sundaramurthy, G. S. Kino, and C. F. Quate, "Optical antennas: resonators for local field enhancement," J. Appl. Phys. **94**(7), 4632 (2003).
12. F. De Angelis, M. Patrini, G. Das, I. Maksymov, M. Galli, L. Businaro, L. C. Andreani, and E. Di Fabrizio, "A hybrid plasmonic-photonic nanodevice for label-free detection of a few molecules," Nano Lett. **8**(8), 2321–2327 (2008).

#142460 - $15.00 USD Received 11 Feb 2011; revised 18 Apr 2011; accepted 3 May 2011; published 9 May 2011

13. M. Barth, S. Schietinger, S. Fischer, J. Becker, N. Nüsse, T. Aichele, B. Löchel, C. Sönnichsen, and O. Benson, "Nanoassembled plasmonic-photonic hybrid cavity for tailored light-matter coupling," Nano Lett. **10**(3), 891–895 (2010).
14. P. Ginzburg, A. Nevet, N. Berkovitch, A. Normatov, G. M. Lerman, A. Yanai, U. Levy, and M. Orenstein, "Plasmonic resonance effects for tandem receiving-transmitting nanoantennas," Nano Lett. **11**(1), 220–224 (2011).
15. J. Li, D. Fattal, and Z. Li, "Plasmonic optical antennas on dielectric gratings with high field enhancement for surface enhanced Raman spectroscopy," Appl. Phys. Lett. **94**(26), 263114 (2009).
16. B. Pettinger, B. Ren, G. Picardi, R. Schuster, and G. Ertl, "Nanoscale probing of adsorbed species by tip-enhanced Raman spectroscopy," Phys. Rev. Lett. **92**(9), 096101 (2004).
17. J. K. Daniels and G. Chumanov, "Nanoparticle-mirror sandwich substrates for surface-enhanced Raman scattering," J. Phys. Chem. B **109**(38), 17936–17942 (2005).
18. W.-H. Park, S.-H. Ahn, and Z. H. Kim, "Surface-enhanced Raman scattering from a single nanoparticle-plane junction," ChemPhysChem **9**(17), 2491–2494 (2008).
19. Y. Chu, M. G. Banaee, and K. B. Crozier, "Double-resonance plasmon substrates for surface-enhanced Raman scattering with enhancement at excitation and stokes frequencies," ACS Nano **4**(5), 2804–2810 (2010).
20. T. Ohno and S. Miyanishi, "Study of surface plasmon chirality induced by Archimedes' spiral grooves," Opt. Express **14**(13), 6285–6290 (2006).
21. Y. Gorodetski, A. Niv, V. Kleiner, and E. Hasman, "Observation of the spin-based plasmonic effect in nanoscale structures," Phys. Rev. Lett. **101**(4), 043903 (2008).
22. Y. Zou, P. Steinvurzel, T. Yang, and K. B. Crozier, "Surface plasmon resonance of optical antenna atomic force microscope tips," Appl. Phys. Lett. **94**(17), 171107 (2009).
23. D. Wang, T. Yang, and K. B. Crozier, "Optical antennas integrated with concentric ring gratings: electric field enhancement and directional radiation," Opt. Express **19**(3), 2148–2157 (2011).
24. D. W. Lynch and W. R. Hunter, in *Handbook of Optical Constants of Solids*, E. D. Palik, ed. (Academic Press, 1985).
25. A. G. Curto, G. Volpe, T. H. Taminiau, M. P. Kreuzer, R. Quidant, and N. F. van Hulst, "Unidirectional emission of a quantum dot coupled to a nanoantenna," Science **329**(5994), 930–933 (2010).
26. H. Aouani, O. Mahboub, N. Bonod, E. Devaux, E. Popov, H. Rigneault, T. W. Ebbesen, and J. Wenger, "Bright unidirectional fluorescence emission of molecules in a nanoaperture with plasmonic corrugations," Nano Lett. **11**(2), 637–644 (2011).
27. K. G. Lee, X. W. Chen, H. Eghlidi, P. Kukura, R. Lettow, A. Renn, V. Sandoghdar, and S. Gotzinger, "A planar dielectric antenna for directional single-photon emission and near-unity collection efficiency," Nat. Photonics **5**(3), 166–169 (2011).
28. E. M. Purcell, "Spontaneous emission probabilities at radio frequencies," Phys. Rev. **69**, 681 (1946).
29. E. J. Blackie, E. C. Le Ru, and P. G. Etchegoin, "Single-molecule surface-enhanced Raman spectroscopy of nonresonant molecules," J. Am. Chem. Soc. **131**(40), 14466–14472 (2009).

1. Introduction

Surface plasmon resonance (SPR) structures have been widely applied to bridge the mismatch between the optical wavelength and the sizes of nano objects by confinement of optical energy in ultra-small volumes, and to enhance interactions between light and matter by increasing local electric field intensities [1,2]. There are two major categories of fabrication techniques for making SPR nano devices. One is bottom-up techniques such as chemical synthesis of nanoparticle aggregates in colloidal solutions and self-assembled nanoparticles formed by annealing metallic thin films. The other is top-down nanofabrication techniques such as electron beam lithography and focused ion beam milling. Bottom-up techniques have been reported to produce enormous SPR enhancement effects, but are currently limited by randomly distributed device parameters and loosely controlled performance [3–7]. In order to achieve reproducible experimental results, top-down approaches have to be used. However, it is technically difficult to achieve smaller than 10 nm features with current lithographic techniques, which significantly limits the increase in local electric field intensities. For example, the local electric field intensities achieved in paired optical antennas, each consisting of a pair of metallic nanoparticles with a small gap in between, quickly decreases with larger gap sizes [4,8–11]. As a result, reproducible achievement of extremely high enhancement of local electric field intensities and light-matter interactions with precisely controlled fabrication still remains a challenge [12–15].

In this paper, we propose the integration of a vertically oriented optical antenna and a metallic spiral ring grating to address this challenge. The excitation and collection optics with metallic spiral ring gratings are discussed in detail, as they are crucial for vertically polarized SPR resonances. An enhancement factor of local electric field intensity of seven orders of

#142460 - $15.00 USD Received 11 Feb 2011; revised 18 Apr 2011; accepted 3 May 2011; published 9 May 2011

magnitude is predicted compared to planewave illumination, assuming a 1 nm gap between the optical antenna and the surface of the metallic grating. We also estimate the device performance for surface enhanced Raman scattering (SERS), an application that demands highly enhanced local field intensities.

2. Vertically oriented optical antennas and excitation and collection optics

While precise fabrication of sub-10nm in-plane features by lithographic techniques is difficult, a number of methods exist that enable smaller feature sizes in the vertical direction, such as deposition or growth of very thin films and scanning probe techniques. SPR nanoparticles can also be directly laid on top of mirror surfaces, or surfaces with certain SPR features, so that the gap distances between the nano particles and the surfaces are as small as the thicknesses of the to-be-examined molecules etc. in between. The mirror surface here refers to the smooth surface of a highly reflective substrate, which can be a metallic substrate or a substrate with a significantly higher dielectric constant than its surroundings. When a SPR nanoparticle is on top of a mirror surface, the nanoparticle and its mirror image form the two halves of a paired optical antenna. Metallic nanospheres, nanocylinders and tips on top of mirror surfaces have been reported for SERS applications [16–19].

Though the gap sizes between the nanoparticles and mirror images can be very small, the vertical orientation of these devices induces degraded performance when regular optical lenses are used for optical excitation and collection. Reported experimental SERS enhancement factors of gold nanoparticles on metallic surfaces are limited to 10^8 [16–19]. This is explained in Fig. 1, which shows that an optical antenna consisting of a nanoparticle and its mirror image is oriented and mainly polarized in the surface normal direction of the substrate. Both the excitation of SPR resonances and the collection of SPR radiation with a regular microscope objective are inefficient. In Fig. 1(a), a collimated laser beam is focused by a macroscopic objective onto the nanoparticle to excite its SPR resonance, and the same objective is used to collect scattering radiation from the nanoparticle. Assuming a collimated laser beam with a central anti-symmetric electric field profile, which is the same as planewaves and fundamental Gaussian beams, and the laser beam being at normal incidence onto a central symmetric objective, the electric field profile in the focal spot must be central anti-symmetric with respect to the objective axis, and the electric field component in the axial direction must be zero on the axis. Therefore in this configuration, it is impossible to excite the vertically polarized SPR resonance in a vertically oriented optical antenna which is located on the axis of the objective. Figure 1(b) shows that a vertically polarized SPR resonance does not radiate efficiently into a collection objective right above it, but mainly radiates into the lateral directions, and also couples to surface plasmon waves when a metallic substrate is used. To solve the aforementioned problem, in some reported experiments with vertically oriented optical antennas, the objectives were placed in angled directions [16]. However, in angled illumination configurations, the working distances of the objectives are limited by the sizes of the objectives so that the numerical apertures (NA) are moderate and the laser beams are not focused as strongly. In addition, the moderate NAs limit the collection efficiency of the SPR radiation. In some other reported experiments, either the optical antennas or the laser beams were placed off the objective axes so that the vertical polarization components in the focal spots are non-zero [18]. Due to smaller field intensities in the focal spots, the latter approach is also inefficient for both excitation and collection.

#142460 - $15.00 USD Received 11 Feb 2011; revised 18 Apr 2011; accepted 3 May 2011; published 9 May 2011

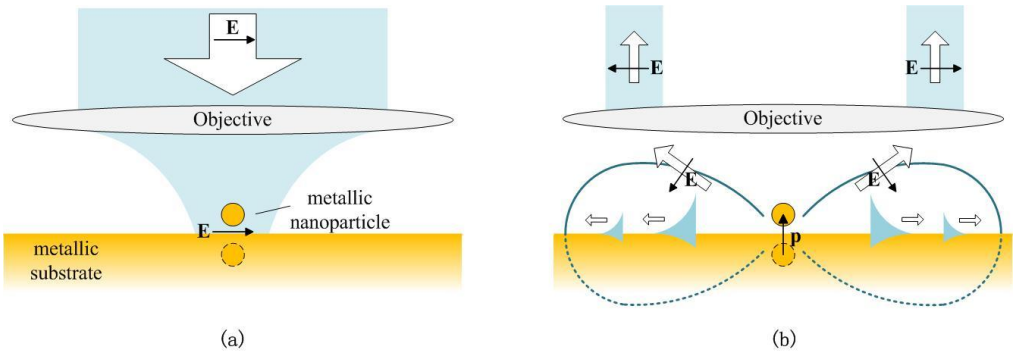

Fig. 1. (a) A collimated and linearly polarized laser beam is focused by a macroscopic objective onto a metallic nanoparticle which is on top of a mirror surface. At the center of the laser focal spot, the electric field is horizontally polarized and can't excite the vertically polarized SPR resonance. (b) A vertically polarized SPR resonance does not radiate efficiently into a collection objective right above, but mainly radiates into the lateral directions and couples to surface plasmon waves.

From the above discussion, it is clear that vertically polarized electric fields at the centers of focal spots are critical for efficient excitation of, and collection from, SPR resonances in vertically oriented configurations. This can be achieved by using central anti-symmetric lenses. While the symmetries of regular macroscopic lenses are difficult to change, there are a variety of focusing and imaging elements the manipulation of whose geometries are straightforward, such as Fresnel zone plates and ring gratings. In the following sections, we numerically investigate the integrated system of a metallic nanosphere and a metallic spiral ring grating, as shown in Fig. 2(a). The spiral ring grating is a central anti-symmetric focusing and collimating element [20,21]. We propose this device structure for the reproducible achievement of large local electric field intensity enhancement and directional radiation. In experiments, the nanosphere could be replaced by other SPR nano devices or be mounted on the tip of a scanning probe for additional functionality [22].

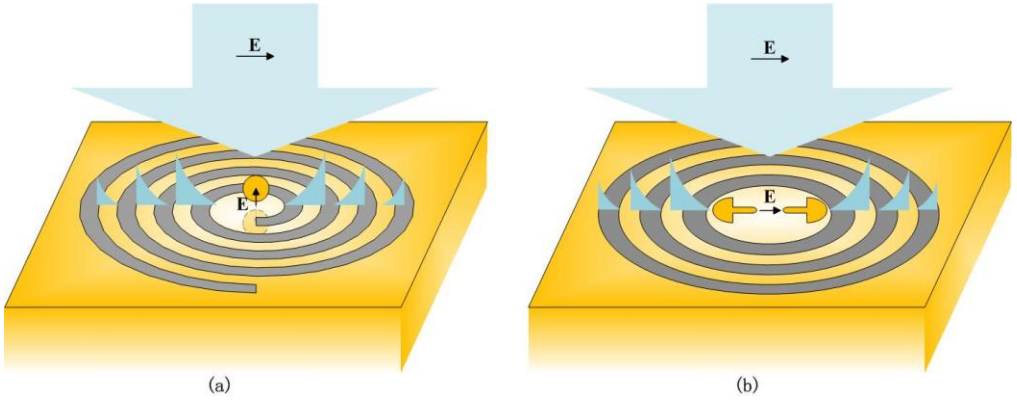

Fig. 2. Schematic illustrations of optical antennas integrated with metallic ring gratings. (a) A metallic nanosphere integrated with a metallic spiral ring grating, with normally incident planewaves concentrated and coupled to vertically polarized antenna resonances. (b) An in-plane paired optical antenna integrated with a metallic concentric ring grating, with normally incident planewaves concentrated and coupled to horizontally polarized antenna resonances.

3. Large enhancement of local electric field intensities in metallic nanospheres integrated with metallic spiral ring gratings

In this section and the following section, we apply the Finite Element Method (FEM) to numerically study the performance of a metallic spiral ring grating for excitation and

#142460 - $15.00 USD Received 11 Feb 2011; revised 18 Apr 2011; accepted 3 May 2011; published 9 May 2011

collection, the local electric field intensity enhancement for a metallic nanosphere integrated with the metallic spiral ring grating, and the SERS electromagnetic enhancement factor of the proposed device. Due to limited computer memory on our 24-core parallel processor, the tetrahedral meshes in our simulations have grid sizes which are larger than one tenth of wavelength in the parts away from the focal spot. We have confirmed that the large grid sizes do not lead to large errors in the simulation results, by comparing simulation results for smaller but similar structures with different grid sizes.

The numerical calculations in this paper follow an earlier piece of work in which we reported the integration of an in-plane optical antenna with a silver concentric ring grating, which is briefly summarized in the following [23]. In Ref. [23], as shown in Fig. 2(b), an incident optical planewave is concentrated by a silver concentric ring grating to a sub-wavelength surface plasmon focal spot at the grating center. The surface plasmon field at the center of the focal spot is horizontally polarized. An in-plane paired optical antenna is placed at the center of the grating and excited by the surface plasmon focal spot. When the in-plane optical antenna has a gap of 10 nm, a local electric field intensity enhancement factor of more than four orders of magnitude is numerically obtained at the center position of the gap. Radiation from the SPR resonance of the antenna is collimated by the ring grating to power density full-width half-maximum (FWHM) angles of less than 10°, which facilitates efficient collection. A SERS electromagnetic enhancement factor of up to eight orders of magnitude is predicted when we assume planewave illumination and a collection NA of 0.7.

In order to obtain a vertically polarized focal spot, we will use a spiral ring grating instead of a concentric ring grating, the latter giving zero electric field in the vertical polarization at the center of the focal spot. The metallic spiral ring grating considered in this paper is illustrated in Fig. 3. The grating is engraved into the flat surface of a gold substrate, with the raised part (the rings) defined by the Archimedean spiral equations:

$$r_{in}(\theta) = \frac{p}{2\pi}\theta + \frac{p}{2}$$
$$r_{out}(\theta) = \frac{p}{2\pi}\theta + p \qquad (1)$$

where $r_{in}(\theta)$ and $r_{out}(\theta)$ are the inner and outer radii of rings at different azimuthal angles, respectively. p is grating period. $\theta \in [0.5\pi, 10.5\pi]$, i.e., there are five rings. The optical properties of gold are taken from Ref. [24]. Above the gold substrate is free space. A y-polarized optical planewave is normally incident along the $-z$ direction.

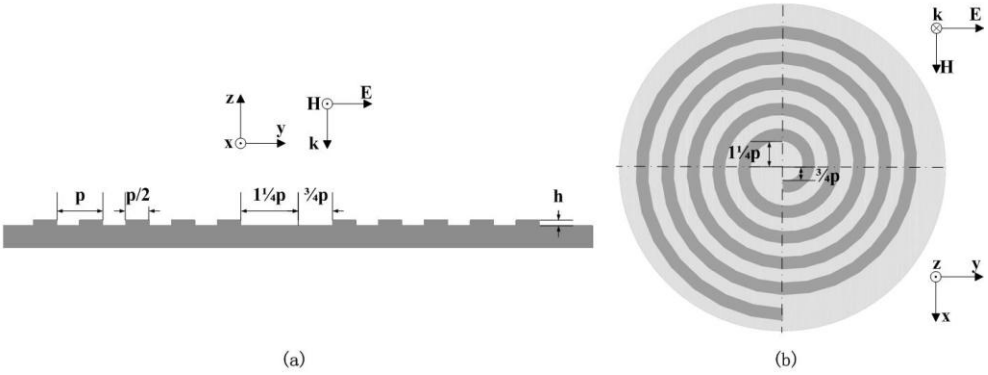

Fig. 3. (a) Cross section of a metallic spiral ring grating. E and H denote the electric and magnetic fields of a y-polarized planewave at normal incidence. (b) Top view of a metallic spiral ring grating. Dark color is raised part (the rings).

Figure 4 presents FEM calculation results of how the normally incident optical planewave is coupled by the gold spiral ring grating to surface plasmons that propagate along the gold

#142460 - $15.00 USD Received 11 Feb 2011; revised 18 Apr 2011; accepted 3 May 2011; published 9 May 2011

surface, and then focused to a z-polarized focal spot at the center of the grating. Figure 4(a) shows the normalized intensity of z-component of electric field (normalized to planewave illumination), $|E_z|^2$, right above the gold surface at the center of the grating ($r = 0$). For a range of grating periods, $|E_z|^2$ is enhanced by around two orders of magnitude in a wavelength bandwidth of almost 100 nm. Figure 4(b) shows an instantaneous z-component of the electric field, E_z. Grating focusing is optimal when the grating period matches the wavelength of surface plasmon wave.

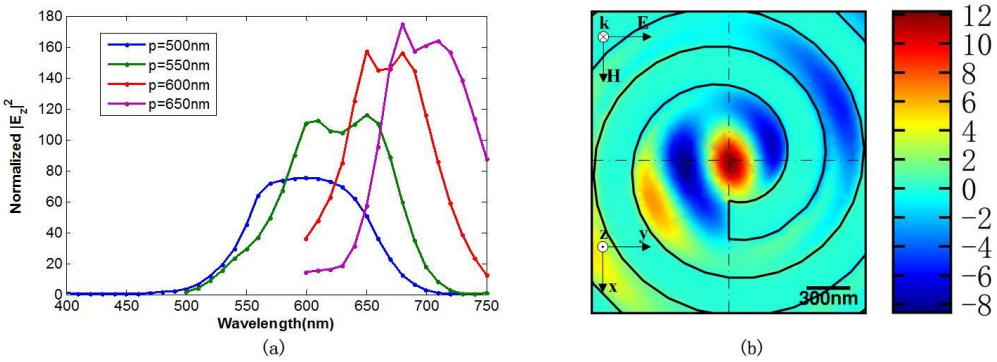

Fig. 4. Fields in gold spiral ring gratings under normally incident *y*-polarized planewaves. All field values are taken at 0.5 nm above the unraised surface of gold substrate, and have been normalized to the incident fields. The thickness of the rings, *h*, is 60nm. (a) $|E_z|^2$ at the center ($r = 0$) of the gratings, for a range of grating periods, *p*, and a range of incident planewave wavelengths. (b) An instantaneous profile of E_z, when p = 600nm and the incident planewave wavelength is 660nm.

We next consider what happens when we place a gold nanosphere at the center of the gold spiral ring grating and 1 nm above the gold surface, as shown in Fig. 5(a). The nanosphere and its mirror image form a vertically oriented paired optical antenna. When the resonance wavelength of the optical antenna matches the wavelength for which focusing by the grating is optimal, the E_z component of the surface plasmon focal spot (Fig. 4(b)) excites the SPR resonance of the optical antenna, which is also *z*-polarized. Due to the tiny gap size of the optical antenna, an enormous increase in local electric field intensity in the gap is achieved. Figure 5(b) shows the normalized $|E_z|^2$ for gold nanospheres integrated with gold spiral ring gratings for normally-incident plane wave illumination. Figure 5(c) shows an instantaneous profile of E_z in the *y*-*z* plane. A simulation grid size of 0.1 nm is used in the 1nm gap. The numerical results in Fig. 5 confirm that the SPR resonance field of the vertically oriented optical antenna is tightly confined within the 1 nm gap, and that a seven orders of magnitude increase in local electric field intensity can be achieved on resonance. In these calculations, the source is launched in a spatially-limited calculation window, meaning that, strictly speaking, it is not a plane wave. In the next section, we use a dipole radiation calculation, which by reciprocity [23] gives a slightly larger enhancement for the perfect plane wave illumination case than what is predicted in Fig. 4. The electric field enhancement factors we simulate for the device we propose are much greater than those achieved in in-plane optical antennas integrated with concentric ring gratings, as these are limited to having larger gap sizes [23]. The enhancement factors are also significantly greater than gold nanospheres on flat gold surfaces (without gratings) under plane wave angled incidence, as shown in Fig. 5(b).

#142460 - $15.00 USD Received 11 Feb 2011; revised 18 Apr 2011; accepted 3 May 2011; published 9 May 2011

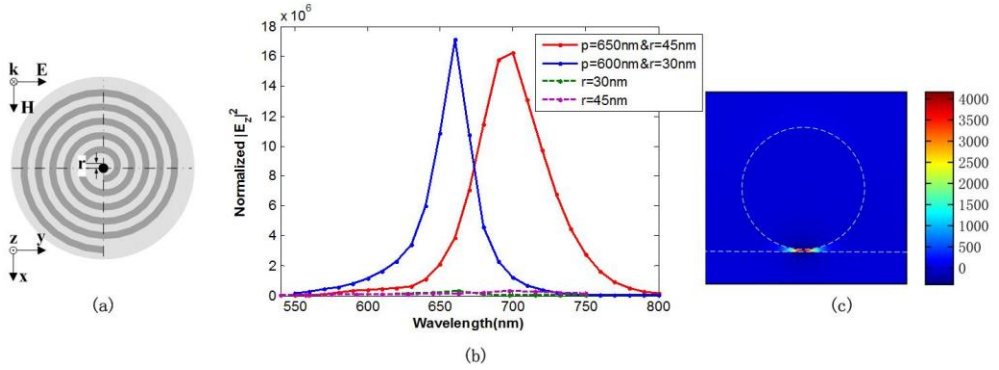

Fig. 5. (a) A gold nanosphere is integrated at the center of a gold spiral ring grating and 1 nm above the unraised surface of gold substrate. (b) Normalized $|E_z|^2$ at the center point of the gap between the nanosphere and the substrate surface, for different grating periods p, sphere radii r, and a range of incident wavelengths. Solid lines: nanospheres integrated with spiral ring gratings are excited by y-polarized plane waves at normal incidence. Dashed lines: nanospheres on flat gold surfaces are excited by planewaves at 45° incidence, with the plane waves being linearly polarized in the plane of incidence. The thickness of the rings, h, is 60nm. (c) An instantaneous profile of normalized E_z in the y-z plane, for a gold nanosphere integrated with a gold spiral ring grating under a normally incident y-polarized planewave. The parameters of the grating are p = 600nm, h = 60nm. The radius of the nanosphere is r = 30nm. The incident planewave wavelength is 660nm.

4. Directional radiation from metallic nanospheres integrated with metallic spiral ring gratings

When the surface plasmon wavelength matches the grating period, the metallic spiral ring grating not only couples normally incident optical illumination to surface plasmon waves, but also collimates the surface plasmon waves radiated by the vertically polarized optical antenna to directional optical radiation into free space. Radiation can also be understood as a reciprocal process to excitation [23]. Directionality facilitates efficient collection of optical antenna radiation [25–27]. Following Ref. [23], an oscillating z-polarized point dipole is placed at the center point of the gap between the nanosphere and the substrate surface to simulate the radiation. The oscillation frequency of the point dipole matches the resonant frequency of the optical antenna and the corresponding surface plasmon wavelength matches the grating period. Figure 6 shows the far-field radiation patterns with and without the spiral ring grating. With an objective of NA = 0.7 placed right above the nanosphere, the collection efficiency is calculated to be as large as 68% for a nanosphere integrated with a grating since radiation is collimated along the z direction, only 13.3% for a nanosphere on a flat gold surface since radiation is mainly into the lateral directions, and 13.7% for a nanosphere on a flat gold surface but with the objective inclined at an angle of 45°. Collection efficiency here is defined as power collected by the objective divided by the total radiated power in the far field. Energy dissipation via metallic ohmic loss is significant in SERS devices, which has not been included in the preceding definition of collection efficiency.

#142460 - $15.00 USD Received 11 Feb 2011; revised 18 Apr 2011; accepted 3 May 2011; published 9 May 2011

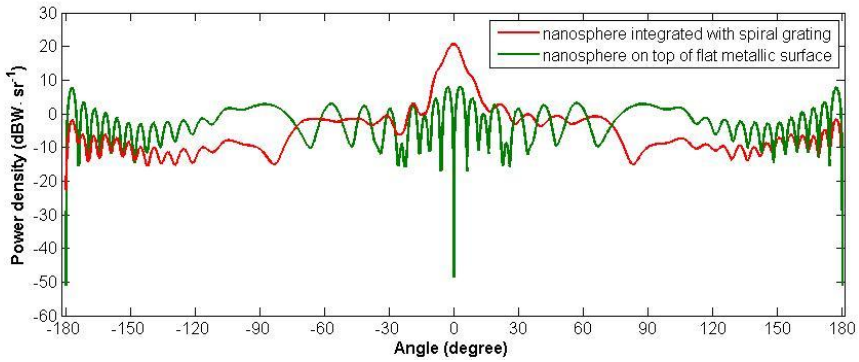

Fig. 6. Far-field radiation patterns of an oscillating point dipole in the *yz* plane. The horizontal axis is the angle between the observation direction and the *z* direction. In the vertical axis, sr means stereoradian. The dipole is *z*-polarized and placed at the center of a 1 nm gap between a gold nanosphere and the surface of a gold plate substrate. Red line: the gold nanosphere is integrated with a gold spiral ring grating. Green line: the gold nanosphere is on top of the flat surface of a gold plate substrate. The periodic ripples are interference arising from the finite size of the gold plate substrate. The device parameters and wavelength are the same as in Fig. 5(c).

The powers radiated by oscillating dipoles are enhanced when the dipoles are coupled to SPR resonances, which is attributed to the Purcell effect [23,28]. With the same device and wavelength as in Fig. 6, a collection objective of NA = 0.7 right above the device, the collected radiation power from a point dipole under a gold nanosphere integrated with a gold spiral ring grating is 7.3×10^5 times higher than a horizontally polarized point dipole in free space with the same dipole moment. The SERS electromagnetic enhancement factor is the product of the enhancement of excitation electric field intensity and the enhancement of collected radiation power. This factor is 1.9×10^{13} when Stokes shift is assumed to be zero, and 3.6×10^{11} when Stokes shift is assumed to be 2000 cm^{-1} (excitation at 660nm and radiation at 760nm). According to a recent analysis, when combined with typical chemical enhancement effects, the magnitude of this electromagnetic enhancement factor shall be sufficient for non-resonant single molecule Raman spectroscopy for some molecules with the smallest Raman scattering cross sections [29].

5. Conclusion

We have proposed integration of vertically oriented optical antennas and metallic spiral ring gratings. By efficient coupling between vertically polarized local SPR resonances in optical antennas and surface plasmon waves on metallic spiral ring gratings, the proposed devices is predicted to produce enormous enhancement in local electric field intensities in the tiny optical antenna gaps under resonant illumination. Radiation from dipoles within the optical antenna gaps are also greatly enhanced and collimated under resonant conditions. With reproducible achievement of large field intensity enhancement and efficient collection, we expect the proposed device structure to be a useful tool for studying and implementing strong light-matter interactions, such as single molecule Raman scattering spectroscopy, single photon sources, etc.

Acknowledgments

We acknowledge fruitful discussion with Dr. Ethan Schonbrun who is currently at the Rowland Institute. B.L., C.S. and T.Y. acknowledge support from the Shanghai Pujiang Program under grant # 10PJ1405300 and the Program for New Century Excellent Talents in University by the Ministry of Education of China. D.W and K.C. acknowledge support from the Defense Advanced Research Projects Agency (grant # FA9550-08-1-0285) and the National Science Foundation (CAREER award, grant # ECCS-0747560).

#142460 - $15.00 USD Received 11 Feb 2011; revised 18 Apr 2011; accepted 3 May 2011; published 9 May 2011